Solution State Characterization of Amyloid β-Derived Diffusible Ligands

Robert W. Hepler,*,‡ Karen M. Grimm,‡,§ Deborah D. Nahas,‡ Robert Breese,|| Elizabeth Chen Dodson,|| Paul Acton,|| Paul M. Keller,‡ Mark Yeager,‡ Hui Wang,‡ Paul Shughrue,|| Gene Kinney,|| and Joseph G. Joyce‡

Department of Vaccine & Biologics Research and Department of Alzheimer's Research, Merck Research Laboratories, West Point, Pennsylvania 19486

Received September 5, 2006; Revised Manuscript Received October 30, 2006

ABSTRACT: A growing body of evidence suggests that soluble oligomeric forms of the amyloid β peptide known as amyloid-derived diffusible ligands (ADDLs) are the toxic species responsible for neurodegeneration associated with Alzheimer's disease. Accurate biophysical characterization of ADDL preparations is hampered by the peptide's strong tendency to self-associate and the effect of factors such as ionic strength, temperature, and pH on its behavior. In addition, amyloid peptides are known to interact with common laboratory excipients, specifically detergents, further complicating the results from standard analytical methods such as denaturing polyacrylamide gel electrophoresis. We have studied the solution behavior of various amyloid peptide preparations using analytical ultracentrifugation and size exclusion chromatography coupled with multiangle laser light scattering. Our results indicate that ADDL preparations exist in solution primarily as a binary mixture of a monomeric peptide and high-molecular mass oligomers. We relate our findings to previously described characterizations utilizing atomic force microscopy and electrophoretic methods and demonstrate that low-molecular mass oligomers identified by gel electrophoresis likely represent artifacts induced by the peptide's interaction with detergent, while atomic force microscopy results are likely skewed by differential binding of monomeric and oligomeric peptide species. Finally, we confirm that only the high-molecular mass oligomeric components of an ADDL preparation are capable of binding to subpopulations of primary hippocampal neurons in vitro.

The amyloid β peptide (Aβ) is produced by proteolytic cleavage of amyloid precursor protein (APP) and is found in vivo primarily as a 39−43-residue peptide. Accumulation of Aβ, particularly the 42-amino acid form [Aβ(1−42)], leads to the formation of large, insoluble deposits (plaques) of aggregated peptide in the brain of patients with Alzheimer's disease (AD) (*1*). It is this plaque deposition that is a hallmark in the post mortem analysis of the AD brain. The "amyloid cascade hypothesis" postulates that a time-dependent deposition of amyloid plaques in the brain is responsible for the neurodegeneration seen in AD (*2*). This hypothesis has been revised in recent years to account for the observation that early neurodegenerative symptoms in AD patients do not necessarily correlate with the onset of plaque deposition. A mounting body of evidence suggests that soluble oligomeric forms of Aβ known as amyloid-derived diffusible ligands (ADDLs) may constitute the acutely toxic peptide species (*3*−*9*). ADDLs have a demonstrated toxicity on neuronal cells in vitro (*10*) and can induce cognitive deficits when administered in vivo (*11*, *12*). Long-term potentiation in hippocampal brain slices is negatively affected by preincubation of the slices with Aβ oligomers (*13*−*15*). The reduction of 3-(4,5-dimethylthiazol-2-yl)-2,5-diphenyltetrazolium bromide (MTT) by cultured cells was shown to be affected by preincubation of the cells with oligomeric Aβ; however, the validity of this assay has been questioned (*16*). It is postulated that the physiological effects of ADDLs may be related to their ability to form ion channels in cell membranes, resulting in membrane depolarization (*17*).

Aβ concentrations in vivo are in the low nanomolar range. This fact, coupled with its propensity to associate with other proteins, has precluded the isolation of large quantities of purified peptide from natural sources. The preparation of ADDLs was first reported by Lambert et al. (*3*), who incubated Aβ(1−42) with clusterin in the presence of components of cell culture media. Subsequently, Stine et al. (*18*) described a preparation method utilizing peptide alone in which synthetic Aβ(1−42) was first dissolved in hexafluoro-2-propanol (HFIP) to eliminate any preexisting secondary structure that could act as a "seed" for aggregation. The HFIP was removed by evaporation, and the dried peptide film was then redissolved in dimethyl sulfoxide (DMSO) and diluted into cell culture medium followed by incubation at 2−8 °C to induce oligomer formation. More recent studies have reported that the HFIP-solubilized peptide may be directly diluted in water followed by evaporation of residual solvent and mechanical agitation to induce oligomer formation (*19*).

Characterization of ADDL preparations has often utilized denaturing polyacrylamide gel electrophoresis (SDS−PAGE), while atomic force microscopy (AFM) and, to a lesser degree, electron microscopy have been successfully used to visualize oligomeric assemblies and distinguish these

* To whom correspondence should be addressed: Department of Vaccine & Biologics Research, WP16-101, Merck Research Laboratories, West Point, PA 19486. Telephone: (215) 652-4786. Fax: (215) 652-7320. E-mail: robert_hepler@merck.com.

‡ Department of Vaccine & Biologics Research.

§ Current address: Acologix, Inc., 3960 Point Eden Way, Hayward, CA 94545.

|| Department of Alzheimer's Research.

10.1021/bi061850f CCC: $33.50
Published on Web 12/06/2006

from monomer and fibrils. Clusterin-derived ADDLs examined by AFM were globular in nature; however, peptide prepared in the absence of clusterin tended to be more fibrillar in nature (*3*). The globules were shown to have a diameter of approximately 3.8−4.7 nm, which was theorized to correspond to a protein of 17000−42000 Da. Further support for the low-mass oligomer structure of ADDLs was provided by nondenaturing electrophoresis where bands were observed at predicted masses of 17 000 and 27 000 Da. Size exclusion chromatography (SEC), analytical ultracentrifugation (AU), and fluorescent dye binding have also been utilized in characterizing the components of this complex system, although to a much more limited degree. In 2003, Chromy et al. (*6*) characterized ADDL preparations using AFM, nondenaturing electrophoresis, and SEC to separate ADDLs into two distinct peaks. They found the preparation to be composed of two species, an early-eluting high-mass component and a more retained low-mass component. They further showed that while the higher-mass peak exhibited punctate binding to primary neurons, the lower-mass peak (estimated to be approximately 13 000 Da) did not bind.

In this study, we sought to provide a definitive profile of the solution state of various forms of the Aβ peptide and to resolve the discrepancies between gel-based and solution-based methods of analysis. Toward this end, we utilized SEC coupled with multiangle laser light scattering detection (SEC/MALLS) and AU to characterize the solution behavior of monomeric peptide, ADDLs, and fibrils. Importantly, we provide definitive evidence using MALLS that previous reports identifying the low-molecular mass component as being composed of low-*n* oligomers are in error, that this species actually represents monomeric peptide, and that the high-molecular mass components are a polydisperse mixture of oligomeric species with molecular masses significantly higher than those previously proposed. We show definitively that intermediate-sized oligomers, postulated by gel-based analyses to be the major component of ADDL preparations, actually represent an insignificant mass of the total peptide in solution and are likely detergent-induced or detergent-stabilized artifacts.

EXPERIMENTAL PROCEDURES

Peptides and Reagents. Aβ(1−42) and Aβ(1−40) peptides along with their N-terminal biotinylated analogues were purchased from American Peptide Co. (Sunnyvale, CA) at purity levels of >95%. 1,1,1,3,3,3-Hexafluoro-2-propanol (HFIP) and anhydrous DMSO were purchased from Sigma-Aldrich (St. Louis, MO). Polyacrylamide gels, buffers, SYPRO-Ruby protein stain, and electrophoresis equipment were purchased from Invitrogen (Carlsbad, CA).

ADDLs were prepared using slight modifications of previously described methods (*20*). Fibrils were prepared as described previously (*18*) by dissolving 0.5 mg of Aβ(1−42) peptide in 1 mL of 10 mM hydrochloric acid and incubating the mixture at 37 °C for 16−18 h. Alternatively, peptide was dissolved to a concentration of 5 mM in DMSO, diluted to 0.5 mg/mL in phosphate-buffered saline, and incubated at 37 °C for 16−18 h. Aβ monomer was prepared by dissolving 0.5 mg of HFIP-treated Aβ(1−40) or Aβ(1−42) in 1.0 mL of 25 mM sodium tetraborate (pH 8.5). These preparations were either used immediately [Aβ(1−42)] or flash-frozen and stored at −70 °C [Aβ(1−40)]. Biotinylated ADDLs (bADDLs) and monomer were prepared by the same protocols using N-terminally biotinylated peptides.

Chromatography. Size exclusion chromatography was performed on an Agilent (Wilmington, DE) 1100 series HPLC system equipped with a diode array detector, a Wyatt Technology (Santa Barbara, CA) Optilab DSP interferometric refractometer, and a Wyatt DAWN EOS multiangle laser light scattering (MALLS) detector. Wyatt Astra software (version 4.90.07) was used to analyze all light scattering data. The refractive index increment for monomeric Aβ(1−42) was determined empirically using flow injection analysis of HFIP-treated peptide. Chromatographic separations were performed in 25 mM sodium phosphate (pH 7.3) at a flow rate of 0.5 mL/min on a 10 mm × 30 cm Superdex 75 column (Amersham Biosciences, Piscataway, NJ) preceded by a 5 mL guard column composed of prep grade Superdex 75. The column was run at room temperature, while the refractometer and light scattering cells were kept at 35 °C.

Large-scale ADDL preparations were separated on a high-resolution 1.6 cm × 60 cm Sephacryl S-200 column (Amersham Biosciences) run in 25 mM sodium phosphate (pH 7.3) at a flow rate of 0.5 mL/min. Five-minute fractions were collected on ice, and the peaks were pooled on the basis of the absorbance at 205 nm.

Analytical Ultracentrifugation. Sedimentation velocity experiments were performed at 4, 20, and 30 °C on a Beckman (Fullerton, CA) XLI analytical ultracentrifuge using an An-60 Ti rotor and double-sector cells. Rotor speeds ranged from 20 000 to 50 000 rpm, and the sample absorbance was monitored at 280 nm for samples prepared in DMSO/F12 or at 215 nm for fractionated SEC peaks in phosphate buffer. Time derivative analysis was performed using the Beckman XLI data analysis software and DC/DT+ software (*21*, *22*). Sedimentation equilibrium experiments were performed on Aβ(1−42) ADDL preps at 476, 238, and 151 μg/mL using six-channel cells. Experiments were performed at 4 °C at speeds of 10 000, 15 000, 20 000, 30 000, and 34 000 rpm. For Aβ(1−40) peptide prepared following the ADDL protocol, measurements were taken at sample concentrations of 476 and 238 μg/mL at a rotor speed of 35 000 rpm. Samples were centrifuged for 20 h before equilibrium absorbance measurements were taken. Molecular masses were calculated using Beckman XLI data analysis software.

Gel Electrophoresis. SDS−PAGE was performed using Novex (Invitrogen) 10 to 20% Tricine gels, along with a Novex sample, and running buffers.

Atomic Force Microscopy. Atomic force microscopy was performed essentially as described previously (*3*, *23*) using a MultiMode atomic force microscope (Digital Instruments/Veeco Metrology, Santa Barbara, CA) controlled by a NanoScope IIIa with NanoScope Extender electronics and Q-Control (nanoAnalytics, Münster, Germany). NanoScope operating software version 4.31 was used to acquire the data images, and Nanoscope offline software was used to render the data and perform the particle and section analyses after zero-order flattening of the image background. The *z*-height of >50 globules from several different areas on the mica was measured. Particle analysis was performed by choosing a threshold height equivalent to $^1/_2$ the average *z*-height of

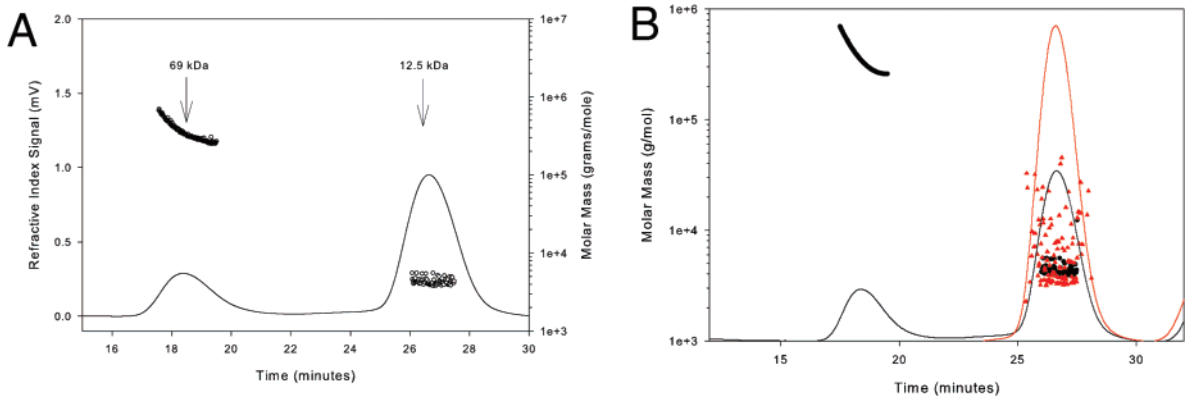

FIGURE 1: (A) Refractive index trace of a standard ADDL preparation with an overlay of the actual molecular mass as calculated by MALLS using an empirically determined dN/dC of 0.241. (B) SEC−MALLs comparison of Aβ(1−42) (black circles) and Aβ(1−40) (red triangles) prepared using the standard ADDL preparation method.

the globules. This measures globule diameter at fwhm (full width at half-maximum).

Primary Neurons. Primary hippocampal cultures were prepared from in-house frozen isolated rat hippocampal cells or commercial frozen dissociated rat hippocampal cells (Cambrex, East Rutherford, NJ) that were thawed and plated according to the manufacturer's protocol in 96-well plates (Corning Costar, Acton, MA) at a concentration of 20 000 cells per well. The cells were maintained in Gibco Neurobasal medium without L-glutamine, supplemented with B27 (Invitrogen) for a period of 2−3 weeks before being used for binding studies.

Neuronal Binding of the High- and Low-Molecular Mass Fractions of ADDLs. Neuronal binding of the high- and low-mass components of a bADDL preparation was investigated as described below by incubating cells with the high- and low-mass peaks of a bADDL preparation that had been isolated by SEC and adjusted to a concentration of 5 μM to match the protein concentration of the unfractionated bADDL control. Primary hippocampal neurons (cultured for 14−21 days) were incubated with 5 μM bADDLs or fractionated bADDL components for 1 h at 37 °C, and then the cells were washed three or four times with warm culture media [Gibco Neurobasal medium without L-glutamine, supplemented with B27 (Invitrogen)] to remove unbound peptide or oligomers. The cells were then fixed with 4% paraformaldehyde diluted in PBS (Electron Microscopy Sciences, Fort Washington, PA) for 10 min at room temperature. This solution was then removed, and fresh fixative was added for an additional 10 min at room temperature. The cells were then permeabilized in 4% paraformaldehyde and 0.1% Triton X-100 (Sigma Aldrich) for 10 min, washed six times with PBS, and incubated for 1 h at 37 °C with blocking buffer [PBS with 10% bovine serum albumin (BSA), Sigma]. For the detection of bADDL binding, the cells were incubated overnight with a 1:1000 dilution of a polyclonal antiserum raised against tau (Sigma Aldrich). The following morning, the cells were washed three times with PBS and incubated for 1 h at room temperature with an Alexa 488-labeled anti-rabbit secondary and an Alexa 594-labeled streptavidin (1:1000 and 1:500, respectively, in PBS with 1% BSA) (Invitrogen), washed five or six times in PBS, and then visualized with a fluorescence microscope. Cell nuclei were labeled with a 1:1000 dilution of DAPI (Invitrogen) following standard protocols. To detect bound bADDLs with monoclonal antibodies, cells were incubated overnight with an anti-ADDL monoclonal antibody (ACU-914, Acumen Pharmaceuticals, Inc., South San Francisco, CA), and in the morning, the immunoreactivity was detected with an Alexa 488-labeled anti-mouse secondary antibody. Bound bADDLs were visualized with an Alexa 594-labeled streptavidin, and the nuclei were stained with DAPI.

RESULTS

Biophysical Characterization of Amyloid Peptide Preparations

Solution State Analysis. A primary objective of this study was to accurately characterize the solution state behavior of amyloid peptide formulations and determine how these data compared with previously reported analyses. To assess the size distribution of ADDLs, we employed SEC (a widely accepted method for size-based determinations), coupling it with laser light scattering detection, which allowed for precise determination of molecular masses. Figure 1A shows a representative refractive index trace of an ADDL preparation, which resolves into two distinct peaks. We marked the column with cytochrome *c* (M_w = 12 500 Da) and bovine serum albumin (M_w = 69 000 Da), and the elution position of these proteins is indicated above the chromatogram. When calibrated against these markers, the ADDL-related peaks have predicted molecular masses of 12000−15000 Da (t_R = 27 min) and 65000−80000 Da (t_R = 18 min). In contrast, the absolute mass determination made by multiangle laser light scattering indicates that the 27 min peak has an actual mass of approximately 4500 Da and thus represents monomeric peptide, while the 18 min peak is a polydisperse mixture of oligomers ranging in size from 150 000 Da at the trailing edge to nearly 1 000 000 Da at the leading edge of the peak. A very small amount of polydisperse material ranging in size from approximately 9000 to 150 000 Da can be detected between the two main components; however, no definitive peaks are observed in this region.

Whole and fractionated ADDLs were also analyzed by AU, and these data are summarized in Table 1. ADDLs analyzed by sedimentation velocity runs at 4 °C were characterized by the presence of a high-molecular mass component which sedimented early in the run and a low-molecular mass component which did not sediment under the same conditions. Time derivative analysis of the high-

Table 1: Summary of AU and SEC−MALLS Data on the Molecular Masses of Various Amyloid β Preparations

	analytical ultracentrifugation			
	velocity		equilibrium	SEC−MALLS
species	average *S*	estimated M_w (Da)	estimated M_w (Da)	estimated M_w (Da)
Aβ(1−42) ADDLs	8.0	175000	120000−540000	NA[a]
Aβ(1−40) ADDLs	ND	ND	5400	3500−12000
SEC high-molecular mass peak	6.7	223000	ND	150000−1000000
SEC low-molecular mass peak	0.55	4500	ND	4500
Aβ(1−42) fibrils	31	>1000000	ND	ND

[a] Not applicable because SEC separates Aβ(1−42) ADDLs into two distinct peaks.

mass species revealed a unimodal distribution of oligomers that ranged in size from 4 to 12 S with an average sedimentation coefficient of 8 S, corresponding to an estimated molecular mass of 175 000 Da. Analyses performed at 20 and 30 °C showed a shift toward higher average *S* values, suggesting that aggregation was occurring as a function of increasing temperature (data not shown). We were able to achieve sedimentation of the lower-molecular mass component at higher rotor speeds; however, due to its small contribution to the total absorbance, it was difficult to obtain a reliable *S* value for this species. Equilibrium analyses were performed on ADDLs at three concentrations using multiple rotor speeds. A portion of the material in the ADDL preparations reached equilibrium during 10 000 and 15 000 rpm runs and yielded average masses of 120000−540000 Da. However, at higher speeds (20000−34000 rpm), very little of the remaining material reached an equilibrium state, suggesting that the high-mass material was completely sedimented early in the run while the lower-mass species remained in solution.

Since the heterogeneous nature of an ADDL preparation rendered data interpretation and mass assignment by AU inconclusive, we scaled up the SEC fractionation protocol to obtain sufficient material for AU measurements to be made on the individual high- and low-molecular mass species. Since the stability of these fractions was tenuous, care was taken to tightly coordinate isolation with subsequent analysis. An additional benefit of this strategy was that formulation medium components that resulted in high background absorbances when analyzing whole ADDL preparations were removed by the fractionation procedure. The total peptide recovery through the scaled-up SEC separation was 70%, with approximately 10 and 90% recovered in the oligomer and monomer fractions, respectively. AU analysis of fractionated ADDLs confirmed the mass distributions observed using the MALLS data. Sedimentation velocity analysis performed on the oligomer fraction yielded an average sedimentation coefficient of 6.7 S with an estimated mass of 223 000 Da. The overall distribution was broad, ranging from approximately 3 to 11 S, again suggesting that a polydisperse population of oligomers is present in this peak. One significant observation from this analysis was the absence of any nonsedimenting material at *S* values of <1, which was routinely observed for unfractionated ADDLs. Velocity analysis of the low-molecular mass component yielded a sedimentation coefficient of 0.55 S with a corresponding calculated mass of 4500 Da, supporting the conclusion drawn from the MALLS data that this species is primarily monomeric Aβ(1−42). For the sake of comparison, we used the less aggregation prone Aβ(1−40) peptide as the starting material for a standard ADDL preparation, and Figure 1B presents the SEC−MALLS analysis of this preparation. The profile is quite distinct from that of ADDLs prepared from Aβ(1−42) in that there is no significant peak observed in the region of the chromatogram associated with soluble oligomers (t_R = 16−18 min). Instead, the major peak (t_R = 27 min) coelutes with the monomer-associated peak of Aβ(1−42) ADDLs. The MALLS data for this species exhibited a high degree of variability, suggesting that Aβ(1−40) exists in a dynamic equilibrium of monomer and dimer under these conditions. Sedimentation velocity analysis of this preparation revealed a single low-mass species that sedimented at high rotor speeds, and equilibrium conditions yielded an average mass of 5400 Da, again slightly higher than the predicted mass of 4330 Da for monomeric Aβ(1−40), suggesting the existence of a monomer−dimer equilibrium for this peptide in solution. To address whether the heterogeneous oligomeric component of ADDLs differed significantly from fibrillar species, Aβ(1−42) fibrils were prepared by published protocols and analyzed by both methodologies. SEC−MALLS did not provide useful data for fibrils as near-total sample loss was observed during chromatography, suggesting that the highly aggregated material could not enter the pores of the separation matrix. This supposition was supported by sedimentation velocity determinations that showed only very high-mass species with sedimentation coefficients ranging from 40 to 60 S. The average value of 31 S was much greater than the value of 6.7 S determined for the fractionated oligomer species, though the corresponding calculated mass of more than 1 000 000 Da was observed as the leading edge component of the oligomer peak in the SEC−MALLS analysis of ADDLs.

Atomic Force Microscopy Analysis. AFM has been demonstrated to be an effective tool for distinguishing soluble oligomeric amyloid peptides from highly aggregated fibrils. Consistent with earlier reports, ADDLs (Figure 2A) appear as a field of globular structures approximately 3−5 nm in height. In contrast, monomeric Aβ(1−42) dissolved in DMSO from an HFIP-dried film and adsorbed directly onto the mica chip surface yields a nondescript homogeneous field of protein (data not shown). Figure 2B shows Aβ(1−42) fibrils prepared by the dilute hydrochloric acid protocol. Long strands of accumulated Aβ peptide characterize this image. A highly magnified image of a portion of the fibril preparation is shown in Figure 2C, in which an isolated subunit which appears to correspond to a globular oligomer is seen next to a single fibrillar strand that appears to be composed of nine of these subunits arranged in a helically twisted bundle.

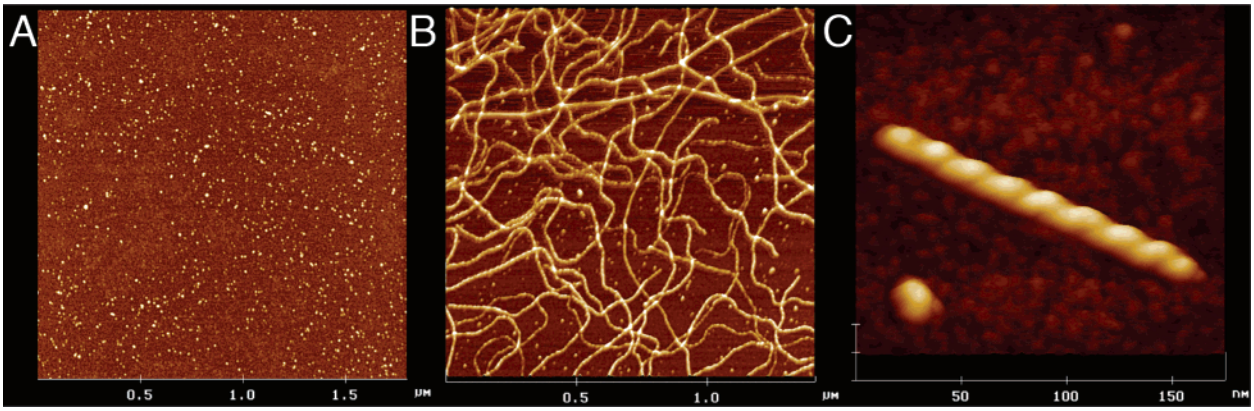

FIGURE 2: Atomic force microscopy was performed on standard preparations of ADDLs (A) and fibrils (B). Panel C is a highly magnified image of a portion of the fibril preparation in which an ADDL subunit is seen next to a structure that appears to be composed of nine of these subunits arranged in a helically twisted bundle. Samples were imaged in air using tapping mode AFM following application of the samples to mica followed by washing and drying.

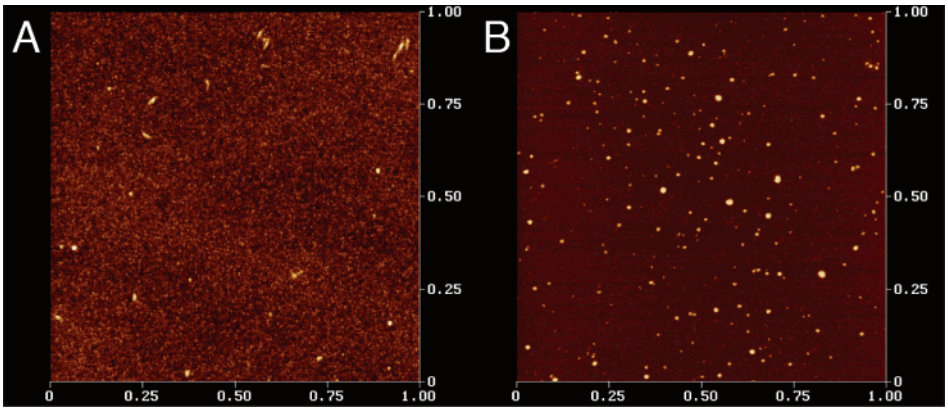

FIGURE 3: AFM images of SEC-fractionated low-mass (Figure 4A) and high-mass (Figure 4B) species isolated from an ADDL preparation by SEC.

Having confirmed that AFM could effectively distinguish the three major peptide structural forms, we next used it to analyze the SEC-fractionated ADDL peaks. As shown in Figure 3, globular structures were observed in both the oligomeric and monomeric fractions. The monomer fraction (Figure 3A) consisted primarily of small globules 2.5 nm in diameter [standard deviation (SD) = 0.9; $n = 230$] and 1.3 nm in height (SD = 0.28; $n = 54$), with little variation in size. A few short fibril-like structures were observed in scans of larger areas, but these were observed relatively infrequently. In contrast, the oligomer fraction (Figure 3B) consisted of much larger globules with an average diameter of 7.8 nm (SD = 3.0; $n = 170$) and 4.5 nm in height (SD = 1.8; $n = 125$). The oligomer-associated structures appeared to contain subpopulations of at least two different size classes with average diameters of 6.1 and 10.3 nm. The 10.3 nm size class was observed with a frequency of approximately 15% of that of the total high-mass globule population. The amyloid globules observed in the monomer fraction were on average 3 times smaller in diameter than globules observed in the high-mass fraction.

No Correlation between Results of SDS−PAGE Analyses and Solution-Based Determinations of ADDL Structure

Denaturing polyacrylamide gel electrophoresis (SDS−PAGE) has been widely used in the literature as a means of characterizing ADDL preparations. We employed this technique to determine how well the results from these analytical methods correlated with the solution state characterizations described above. In Figure 4A, freshly prepared monomeric Aβ(1−42), ADDLs, and fibrils were electrophoresed under denaturing conditions on a Tricine-SDS gel and stained with SYPRO-Ruby. The most striking observation is that all three preparations (ADDLs, monomer, and fibrils) yield virtually identical electrophoretic profiles. The major species identified on the basis of calibration with known molecular mass standards are monomer, trimer, and tetramer, which are clearly visible in all samples. The only apparent difference among the preparations is the appearance of a diffuse high-molecular mass staining associated with the fibril preparation. We performed several additional experiments to try to determine the basis for the discrepancy between SDS−PAGE and SEC−MALLS−AU characterization of ADDLs. One obvious area to consider was the effect of the denaturant on the gel profiles. To address this, samples of an ADDL preparation were diluted to final concentrations of 50, 25, and 5 μM in either F12, 0.05% SDS in water, or 4.0% SDS in water and incubated at room temperature for 1 h. Each sample was then mixed with an equal volume of 2× buffer (containing 8% SDS), immediately loaded onto the gel, and electrophoresed. The results are shown in Figure 4B. All three bands were observed in each sample; however, the distribution of mass in these bands appeared to change depending upon the buffer used during the room-temperature incubation step. ADDLs diluted in F12 medium yield a profile in which similar amounts of peptide are distributed

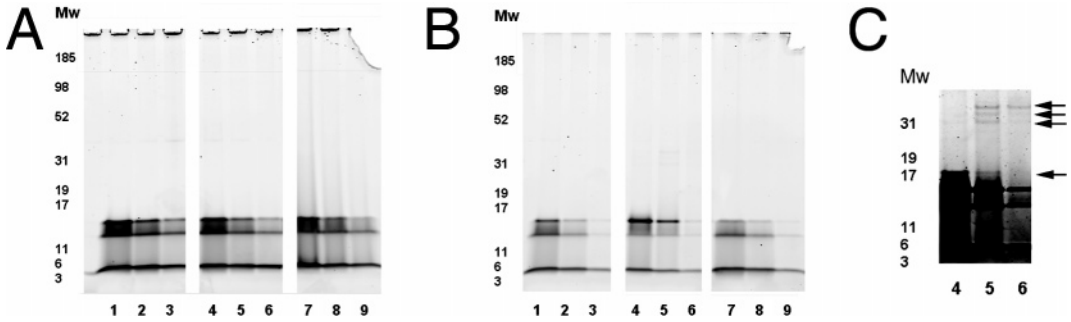

FIGURE 4: (A) Monomeric Aβ(1−42) (5, 2.5, and 1.25 ng in lanes 1−3, respectively), ADDLs (5, 2.5, and 1.25 ng in lanes 4−6, respectively), and fibrils (5, 2.5, and 1.25 ng in lanes 7−9, respectively) were analyzed by SDS−PAGE. The gel was then fixed and stained overnight with SYPRO-Ruby, washed, and imaged with a Typhoon laser imager. (B) A standard ADDL preparation was diluted to 50, 25, and 5 μM in F12 medium (lanes 1−3), 0.05% SDS in water (lanes 4−6), and 2% SDS in water (lanes 7−9) and incubated for 1 h at room temperature. An equal volume of 2× sample buffer was added to all samples, which were immediately loaded (20 μL per lane) and electrophoresed. (C) Deliberate overexposure of lanes 4−6 in panel B showing the presence of additional higher-molecular mass oligomers not found under the other conditions used in this study.

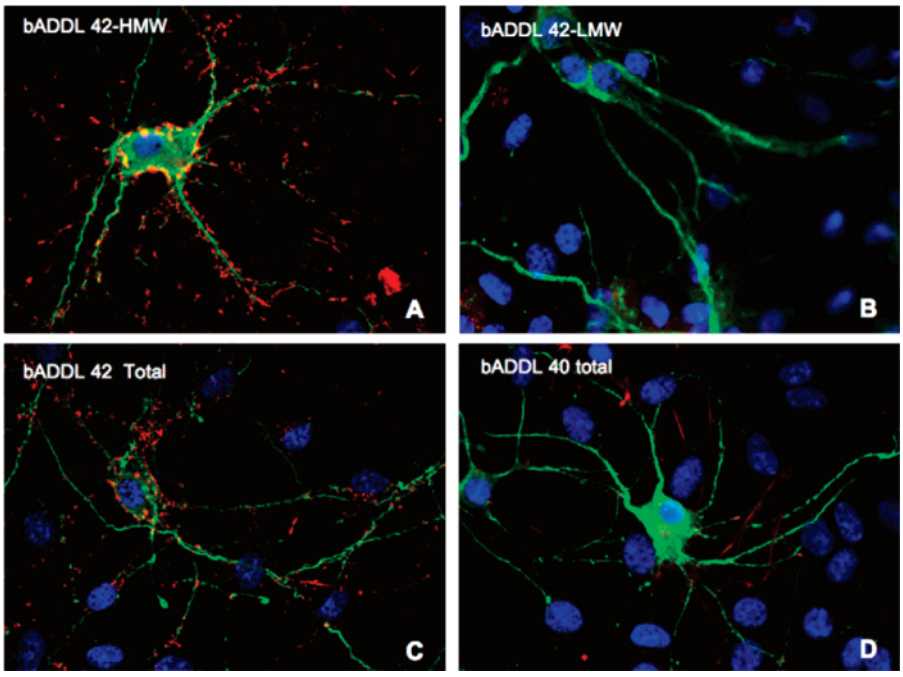

FIGURE 5: Panel C shows the punctate binding of unfractionated bADDLs to the long axonal processes of neurons. SEC-purified high-mass oligomers (A) exhibit a binding pattern very similar to that of unfractionated bADDLs. In contrast, SEC-purified Aβ(1−42) monomer (B) and monomeric Aβ(1−40) (D) exhibit an almost complete absence of staining.

among the three bands, while ADDLs incubated in 0.05% SDS, a concentration below the critical micelle concentration (CMC) of 0.2% for this detergent, yield a distribution which appears to favor formation of tetramer. In addition, incubation of ADDLs with 0.05% SDS results in the appearance of higher-molecular mass SDS-resistant oligomers (Figure 4C). These oligomers consistently appeared in multiple preparations of ADDLs incubated in the presence of 0.05% SDS. Interestingly, when ADDLs were incubated in the presence of 2% SDS, a concentration at which SDS micelles are expected to be present, the distribution of oligomers suggested that monomer and trimer were the favored species, and the higher-order oligomers present in the 0.05% SDS sample were not seen. To determine if SDS exerted an influence on ADDLs in solution, they were preincubated with either 0.1 or 1% SDS and analyzed by SEC in the presence of 0.1 or 1% SDS. Interestingly, in both cases, only a single peak was observed which comigrated with the oligomeric component of non-detergent-treated ADDLs (data not shown). Unfortunately, the presence of SDS prohibited assignment of molecular mass from the MALLS data; however, the colocalization at both SDS concentrations suggests that SDS either effected conversion of monomer to oligomer or associated with monomer in mixed micelles.

Neuronal Binding Is Limited to the High-Molecular Mass Species of an ADDL Preparation

Previously published reports have described the ability of ADDLs to bind to neurons. We sought to determine if both oligomeric and monomeric forms of Aβ(1−42) contained within these heterogeneous preparations contributed to this binding. To accomplish this, we incubated samples of whole and SEC-fractionated bADDLs (5 μM total peptide) with cultured and primary rat hippocampal neurons. Figure 5 shows the results of this analysis. The neuronal nuclei and cell bodies were visualized by differential staining with 4′,6-diamidino-2-phenylindole (DAPI) or a fluorescently labeled monoclonal to total tau protein. Figure 5C shows that

unfractionated bADDLs bind in a punctate manner to the neurons, with the bulk of the biotin reporter detected along the long axonal processes. On average, approximately 30−40% of the total cells within a primary culture are stained. It is of note that all staining appears to be external, and no evidence of internalization of bADDLs is detected under these conditions. A dramatic difference is observed in the binding ability of the SEC fractionated high- and low-mass pools. The high-mass oligomers (Figure 5A) exhibit a pattern very similar to that of unfractionated bADDLs with significant bound biotin detected throughout the field of cells. In contrast, the monomeric Aβ(1−42) fraction exhibits an almost complete absence of staining (Figure 5B). To confirm whether this lack of binding was specific to the Aβ(1−42) peptide or whether it reflected a general inability of monomer to bind, we repeated the experiment using a monomeric preparation of Aβ(1−40), and the result is shown in Figure 5D. Although some spurious fluorescence is detected, the staining is inconsistent with the punctate, regularly stained pattern observed for the oligomer-containing fractions.

DISCUSSION

The amyloid cascade hypothesis proposed in 1992 by Hardy and Higgins (*2*) defined a promising new area for research into the treatment and prevention of Alzheimer's disease. More recent findings, particularly those derived from transgenic animal models in which the onset of cognitive deficiencies precedes the deposition of plaque and neurofibrillary tangles, has necessitated a revisitation of the hypothesis and focused new interest on the role played by ADDLs in the early neurodegeneration experienced by AD patients (*25*, *26*). The majority of characterization and functional studies have been carried out using synthetic peptide since it is readily available in a highly purified form. While synthetic ADDLs have demonstrated neurotoxicity and specific neuronal binding, it is important to realize that the formulation conditions utilized are dramatically different from those encountered in vivo, particularly with respect to the relatively high peptide concentrations used for oligomer formation. Therefore, it is critically important to accurately characterize and understand the nature of ADDLs with respect to what types of species constitute the whole, which are important for mediating biological effects, and the nature of their behavior in solution.

In the current report, we utilized SEC−MALLS and AU to provide an accurate representation of the solution structure of ADDLs. We recognized these techniques as being appropriate for preserving the labile nature of the oligomers while minimizing perturbations to the system caused by the analytical methodology that was used. SEC fractionation of ADDLs and Aβ(1−40) oligomers has been previously described (*6*, *27*). Molecular mass estimates for these peaks based on the use of calibration standards indicated that the early-eluting fraction was in the 75 000 Da range, while the retained fraction was approximately 13 000 Da. We confirmed that the chromatographic separation was reproducible, yielding two well-resolved peaks. However, we recognized that this type of calibration assumes that standards and analyte are structurally similar (i.e., globular, extended rods, spherical) and that differences in molecular shape can have significant effects on migration times. Another potential issue with retention time comparisons is the possibility of nonspecific interaction of the soluble analyte with the solid phase. Under ideal SEC conditions, migration through the column is based on hydrodynamic volume alone. However, hydrophobic proteins and peptides have a tendency to interact with the column matrix, resulting in nonideal elution of analytes from the column. This can be particularly pronounced for Superdex-type resins (*28*). MALLS provided a means for absolute mass determination independent of column-induced migration artifacts. The coupling of SEC and MALLS was critical since conventional dynamic light scattering would have yielded an average population distribution skewed to the high-mass end as a result of the low percentage of very high-mass oligomers (more than 1 000 000 Da) which were identified. A critical observation resulting from this study was identification of the retained species as monomer. The previous assignment of mass suggested that this peak represented tetramer, which was interpreted as a confirmation of gel-based analyses. Furthermore, previous identification of the oligomer species as one comigrating with bovine serum albumin (mass $\sim$ 68 000 Da) predicted a 12-mer multimer, again corresponding to bands sometimes observed via SDS−PAGE (*29*). The MALLS data definitively show that the high-mass component is actually much larger and more polydisperse, constituting a population ranging from approximately 150 000 to more than 1 000 000 Da.

While we felt confident that SEC was a reliable means for assessing the solution state structure of ADDLs, we were still concerned that there was the potential for misinterpretation due to interactions with the column. Therefore, we sought to confirm these results by AU, a technique in which there was no intervening matrix for nonspecific interaction or perturbation of the oligomers. The heterogeneity of unfractionated ADDLs was qualitatively confirmed by AU, although this complexity prevented accurate mass determination even on an average population basis. Nevertheless, we were able to discern the presence of a very low-mass component on the basis of its lack of sedimentation under equilibrium conditions. On the opposite end of the spectrum, the very high-mass nature of fibrils was clearly observable in their rapid sedimentation behavior. It is important to point out that the sedimentation coefficients of fibrils were clearly higher than those of the high-mass components of ADDLs. This suggests that while a continuum consistent with the amyloid cascade hypothesis may exist, the physiological behavior of ADDLs is not the result of small amounts of nascent fibrils. The true correlation between SEC and AU determinations was realized upon analysis of the fractionated species. The low-mass component was unambiguously shown to consist exclusively of monomeric peptide, while estimation of the average mass of the oligomer component showed excellent agreement between methods.

Our findings address another important consideration for interpretation of studies utilizing ADDLs, and that is the demonstration that the system exists in a dynamic equilibrium. Both SEC and AU definitively showed that multiple parameters such as peptide concentration, formulation temperature, storage time, buffer choice, and excipient addition could dramatically affect the distribution of peptide within the continuum. The most relevant of these findings is that an ADDL preparation is not composed exclusively of a defined oligomeric population, as had been suggested by the

aforementioned calibration-derived masses of fractionated components. In fact, greater than 50% of the mass can be ascribed to monomer depending on the formulation conditions that are used. This is critically important in interpretation of toxicity and binding studies. Our results further confirmed the differential aggregation propensities for Aβ(1−42) and Aβ(1−40). While ADDLs exhibited only a quasi-stability, which was limited even at 2−8 °C storage, the 40-mer remained largely monomeric even when prepared under conditions identical to those used for ADDL formulation. Both SEC and AU identified a monomer−dimer equilibrium for Aβ(1−40), but its overall stability was more pronounced than that for Aβ(1−42).

Atomic force microscopy and gel electrophoresis have been widely used to characterize amyloid peptide species, but our findings indicate the need for careful interpretation of these results in light of the solution-based analyses. AFM has proven useful because it can provide a high-resolution image at the molecular level revealing detailed images of protein structures. The technique is most informative for assemblies of regular repeating units such as oligomers, fibrils, and viruses and was the primary analytical method reported for the identification of ADDLs. Lambert et al. (*3*) identified small globular oligomeric structures by studying synthetic Aβ(1−42) incubated with clusterin. These same structures were observed in the absence of clusterin utilizing the HFIP/F12 formulation subsequently described (*6*). In AFM, samples are allowed to bind to the surface of a molecularly flat substrate for subsequent imaging. Muscovite mica and highly ordered pyrolytic graphite (HOPG) are two common substrates, and both have been employed for the study of Aβ peptides (*6*, *30*−*32*), although mica has been used most often for ADDL analysis. Interestingly, studies using HOPG have led to the identification of significantly different structures (*33*, *34*). Aβ(1−42) adsorbed to mica exhibits globular structures (*33*), similar to those reported for ADDLs (*6*) and described in this work. In contrast, when HOPG is used, the peptide forms thin sheets of β structure (*33*, *34*), which suggests that the substrate itself can alter the structure of the samples undergoing analysis. The mechanism(s) responsible for the binding of proteins to substrates has not been fully defined; however, electrostatic and van der Waals forces are thought to be important for binding to mica, while hydrophobic interaction has been proposed as the major mechanism involved in binding to HOPG (*35*). If charge interaction is important for adsorption of ADDLs onto mica, then binding would be expected to depend upon a number of factors such as isoelectric point, the pH and ionic strength of sample buffer, and the nature of any excipients present. Previous AFM studies of ADDLs have not presented data to suggest that all of these factors had been taken into consideration (*6*). For this reason, and because all species in a mixture may not be equally adsorbed to the imaging surface (*36*), extrapolation of the characteristics of mica-bound species to the composite nature of peptide in solution should be done with caution. Given these caveats, we felt it was necessary to directly compare AFM data both to previously reported results and to our solution-based analytical methodologies. Our AFM analyses of fibril, monomer, and intact ADDL preparations show the same characteristic profiles described in previous publications (*6*). Small globular structures 7.8 nm in diameter and 4.5 nm in height appear to be the only species in an ADDL preparation that bind to the mica. Previous studies have suggested that these oligomers have a predicted mass based on diameter of approximately 60 000 Da. However, with AU and SEC, we saw no evidence of this particular structure predominating in solution, suggesting that they either represent a preferentially bound minor solution component or are induced by binding of peptide to the mica surface. The latter explanation seemed less likely given that Aβ(1−40) monomer did not form globules, but this peptide also exhibits a much weaker propensity to self-associate than the 42-mer.

To further address this question, we performed AFM imaging of the SEC-fractionated ADDL components. We observed a highly populated field of globular structures in the oligomer fraction which closely resembled that of an unfractionated ADDL preparation. The lack of a significant amount of larger AFM structures, which would correlate with the masses observed by MALLS and AU in both unfractionated ADDLs and the isolated oligomeric fraction, may reflect an instability of these species to the preparation method. It is less likely that they represent a preferentially adsorbed component due to the relative homogeneity of their profile and the fact that they constitute a negligible portion of the total solution species. Somewhat surprisingly, imaging of the monomeric component also revealed the presence of spherical assemblies, although these were, on average, 3-fold smaller than those seen in the oligomer and unfractionated ADDL samples. These data suggest that structure might be induced by binding of monomeric Aβ(1−42) to surfaces. As noted above, this may be preferentially exhibited by the 42-mer given its stronger propensity to aggregate. Indeed, our SEC stability studies clearly indicated that the propensity to self-associate was considerably greater for Aβ(1−42). However, given our observation that the ADDL preparation contains a significant amount of monomer, it is unclear why these smaller structures are not detected by AFM of unfractionated ADDLs. It may be that in a mixed population of oligomer and monomer, re-equilibration combined with differential binding abilities results in the median-sized globules characteristic of the ADDL preparation.

The solution-based and AFM determinations reported here clearly contrast with results generated by polyacrylamide gel electrophoresis utilizing both denaturing and native conditions, another technique that has been reported extensively in the literature for the characterization of amyloid oligomers, although the value of this technique for characterization of Aβ oligomers has recently been called into question (*37*). SDS−PAGE is a reductive technique and as such cannot provide an accurate reflection of the solution state of noncovalently associated Aβ oligomers. Despite this fact, a fair amount of emphasis has been placed on the lowest-order oligomers observed with this analytical method, and their identification as "building blocks" for higher-order structures. Our current work demonstrates that when monomers, ADDLs, or fibrils are examined on the same gel, all three preparations produce essentially the same banding pattern of monomer, trimer, and tetramer, consistent with multiple published reports. However, solution-based analyses indicate that while a significant portion of an ADDL preparation consists of monomeric peptide, no other lower-order species at the mass values expected for trimer or tetramer are observed, except for a very minor absorbance component

above baseline. The same can be said for fibril preparations, although in this case the SEC data were not informative since the majority of the material in solution is too large to enter the column. The results of SDS−PAGE, SEC−MALLS, and AU correlate best for monomeric Aβ(1−40) which exhibited monomer, dimer, and tetramer bands by gel and evidence of a monomer−dimer equilibrium by SEC and AU, although tetramer was not observed in solution. We evaluated the native PAGE to determine if this method could provide a more appropriate representation of the solution state distribution of peptide forms. The major difficulty with this approach was the lack of suitable calibration standards for calculation of molecular masses. Unlike SDS−PAGE, the migration of proteins under native conditions heavily depends upon the charge, size, and shape of the analyte, and it is difficult to predict which calibration proteins would be appropriate models for analysis of ADDLs. In our hands, ADDLs exhibited two distinct species which migrated with apparent molecular masses of 32 000 and 36000−50000 Da. Incubation of ADDLs at 37 °C resulted in complete replacement of these bands with a more slowly migrating diffusely stained species. While reliable mass estimates could not be obtained, the behavior was consistent with the time- and temperature-dependent conversion of ADDLs to higher-order species that were observed by SEC and AU. Tellingly, when analyzed by SDS−PAGE, these same samples produced an identical banding pattern of monomer, trimer, and tetramer. In an attempt to circumvent some of the uncertainties associated with gel analyses, photoinduced chemical cross-linking has been described as a means of trapping low-mass oligomers in a denaturation-resistant state (*38*). In these studies, intermediate-order multimers ranging from monomer through 12-mers were the most commonly identified species, with differential banding patterns observed for Aβ(1−42) and Aβ-(1−40) preparations. However, the observed masses of these multimers are still inconsistent with solution-based analyses which estimate an average mass of approximately 250 000 Da for the oligomer population.

More importantly, our experiments examining the effect of SDS on band migration patterns strongly suggest that low-order bands such as trimer and tetramer are in fact induced by the detergent. These observations are not inconsistent with the expected behavior of an amphipathic self-associating peptide such as Aβ, and the ability to form mixed micelles with an anionic detergent such as SDS is in agreement with previously described interactions of amyloid peptides with gangliosides (*39*−*44*). Our SEC results provide an independent confirmation of the ability of a detergent to induce structure since addition of either 0.1 or 1% SDS to an ADDL preparation completely converted the residual monomeric peptide to oligomer. Interestingly, incubation of Aβ with SDS at a concentration above its CMC was recently reported to be a useful preparative technique for an oligomeric species termed a "globulomer" (*45*). This preparation was unique in the monodisperse nature of the product and its stability over time. Mechanistically, the formation of mixed micelles of peptide and SDS serving as the basis for further organization into higher-order structures is understandable. However, the current results describing formation of apparently stabilized multimers upon dilution of ADDLs in SDS at sub-CMC concentrations are novel. Whatever the nature of these interactions, there clearly exists a discrepancy between gel-based and solution-based analyses. These findings have important implications for studies beyond those utilizing synthetic peptides since several recent reports describing extraction of "natural amyloid oligomers" from the brains of transgenic animals overexpressing Aβ have relied on SDS−PAGE for identification of conserved 12-mer complexes. In most cases, the rather harsh extraction conditions incorporated use of a solubilizing detergent (*11*, *29*).

The use of biotinylated Aβ for cell binding studies represented an improvement over antibody-based detection in that it allowed direct visualization of bound species and precluded the possibility of nonspecific antibody binding. Our biophysical studies confirmed that biotinylated Aβ(1−42) bADDLs were indistinguishable from ADDLs made using unmodified peptide, while colocalization analyses demonstrated that the two formulations bound the same neuronal targets. Both ADDLs and bADDLs exhibited distinct punctate staining patterns, showing a clear preference for neuronal processes instead of cell bodies. Whether this is indicative of the existence of a specific ADDL receptor is not known. The absolute dependence of the binding interaction on the oligomeric nature of the peptide is clearly demonstrated by the fractionation studies in which the monomeric bADDL component exhibited a complete lack of binding, an observation confirmed using Aβ(1−40) monomer. While similar results have been previously described (*4*, *46*), our data show for the first time that it is monomer and not low-mass oligomers which fails to interact with neurons. While we did not observe killing of these cultured cells, the findings strongly indicate that the only active components of ADDL preparations in MTT-based PC12 toxicity assays are oligomers (*4*). This observation may also provide an explanation for why some agents that prevent oligomerization of the Aβ peptide also prevent Aβ-induced neurotoxicity (*47*−*49*).

In conclusion, we believe that the current study represents an important advancement in the understanding of ADDL solution dynamics. The established picture of ADDLs as an assemblage of low-order Aβ multimers is inaccurate, with the true population constituting a heterogeneous oligomeric component along with a significant amount of residual monomer. Interconversion of forms is possible, and progression to increasingly higher-order structures is influenced by multiple factors. This dynamic behavior must be considered when interpreting the biological effector functions mediated by ADDLs, and particularly with regard to the design of critical assays. We have definitively shown that the interaction of ADDLs with primary hippocampal neurons is mediated exclusively by the oligomeric component of the preparation. Finally, our study points to the caution that must be exercised when attempting to extend the results of non-solution-based methods of analysis to the solution state behavior of proteins and peptides.

ACKNOWLEDGMENT

We thank Dr. Michael J. Allen at Biometrology (Alameda, CA) for atomic force microscopy support and Acumen Pharmaceuticals, Inc., for monoclonal antibodies.

REFERENCES

1. Glenner, G. G., and Wong, C. W. (1984) Alzheimer's disease: Initial report of the purification and characterization of a novel

cerebrovascular amyloid protein, *Biochem. Biophys. Res. Commun. 120*, 885−890.
2. Hardy, J. A., and Higgins, G. A. (1992) Alzheimer's disease: The amyloid cascade hypothesis, *Science 256*, 184−185.
3. Lambert, M. P., Barlow, A. K., Chromy, B. A., Edwards, C., Freed, R., Liosatos, M., Morgan, T. E., Rozovsky, I., Trommer, B., Viola, K. L., Wals, P., Zhang, C., Finch, C. E., Krafft, G. A., and Klein, W. L. (1998) Diffusible, nonfibrillar ligands derived from Aβ1−42 are potent central nervous system neurotoxins, *Proc. Natl. Acad. Sci. U.S.A. 95*, 6448−6453.
4. Lacor, P. N., Buniel, M. C., Chang, L., Fernandez, S. J., Gong, Y. S., Viola, K. L., Lambert, M. P., Velasco, P. T., Bigio, E. H., Finch, C. E., Krafft, G. A., and Klein, W. L. (2004) Synaptic targeting by Alzheimer's-related amyloid β oligomers, *J. Neurosci. 24*, 10191−10200.
5. Gong, Y. S., Chang, L., Viola, K. L., Lacor, P. N., Lambert, M. P., Finch, C. E., Krafft, G. A., and Klein, W. L. (2003) Alzheimer's disease-affected brain: Presence of oligomeric Ab ligands (ADDLs) suggests a molecular basis for reversible memory loss, *Proc. Natl. Acad. Sci. U.S.A. 100*, 10417−10422.
6. Chromy, B. A., Nowak, R. J., Lambert, M. P., Viola, K. L., Chang, L., Velasco, P. T., Jones, B. W., Fernandez, S. J., Lacor, P. N., Horowitz, P., Finch, C. E., Krafft, G. A., and Klein, W. L. (2003) Self-assembly of Aβ(1−42) into globular neurotoxins, *Biochemistry 42* (44), 12749−12760.
7. Klein, W. L., Stine, W. B., and Teplow, D. B. (2004) Small assemblies of unmodified amyloid β-protein are the proximate neurotoxin in Alzheimer's disease, *Neurobiol. Aging 25*, 569−580.
8. Klein, W. L., Krafft, G. A., and Finch, C. E. (2001) Targeting small Ab oligomers: The solution to an Alzheimer's disease conundrum? *Trends Neurosci. 24*, 219−224.
9. Klein, W. L. (2002) ADDLs & protofibrils: The missing links? *Neurobiol. Aging 23*, 231−233.
10. Whalen, B. M., Selkoe, D. J., and Hartley, D. M. (2005) Small non-fibrillar assemblies of amyloid β-protein bearing the Arctic mutation induce rapid neuritic degeneration, *Neurobiol. Dis. 20*, 254−266.
11. Cleary, J. P., Walsh, D. M., Hofmeister, J. J., Shankar, G. M., Kuskowski, M. A., Selkoe, D. J., and Ashe, K. H. (2005) Natural oligomers of the amyloid-β protein specifically disrupt cognitive function, *Nat. Neurosci. 8* (1), 79−84.
12. Rowan, M. J., Klyubin, I., Wang, Q., and Anwyl, R. (2005) Synaptic plasticity disruption by amyloid β protein: Modulation by potential Alzheimer's disease modifying therapies, *Biochem. Soc. Trans. 33* (Part 4), 563−567.
13. Walsh, D. M., Klyubin, I., Fadeeva, J. V., Cullen, W. K., Anwyl, R., Wolfe, M. S., Rowan, M. J., and Selkoe, D. J. (2002) Naturally secreted oligomers of amyloid β protein potently inhibit hippocampal long-term potentiation in vivo, *Nature 416*, 535−539.
14. Nomura, I., Kato, N., Kita, T., and Takechi, H. (2005) Mechanism of impairment of long-term potentiation by amyloid β is independent of NMDA receptors or voltage-dependent calcium channels in hippocampal CA1 pyramidal neurons, *Neurosci. Lett. 391* (1−2), 1−6.
15. Walsh, D. M., Townsend, M., Podlisny, M. B., Shankar, G. M., Fadeeva, J. V., El Agnaf, O., Hartley, D. M., and Selkoe, D. J. (2005) Certain inhibitors of synthetic amyloid β-peptide (Ab) fibrillogenesis block oligomerization of natural Ab and thereby rescue long-term potentiation, *J. Neurosci. 25*, 2455−2462.
16. Wogulis, M., Wright, S., Cunningham, D., Chilcote, T., Powell, K., and Rydel, R. E. (2005) Nucleation-dependent polymerization is an essential component of amyloid-mediated neuronal cell death, *J. Neurosci. 25*, 1071−1080.
17. Demuro, A., Mina, E., Kayed, R., Milton, S. C., Parker, I., and Glabe, C. G. (2005) Calcium dysregulation and membrane disruption as a ubiquitous neurotoxic mechanism of soluble amyloid oligomers, *J. Biol. Chem. 280* (17), 17294−17300.
18. Stine, W. B., Dahlgren, K. N., Krafft, G. A., and LaDu, M. J. (2003) In vitro characterization of conditions for amyloid β peptide oligomerization and fibrillogenesis, *J. Biol. Chem. 278*, 11612−11622.
19. Kayed, R., Sokolov, Y., Edmonds, B., McIntire, T. M., Milton, S. C., Hall, J. E., and Glabe, C. G. (2004) Permeabilization of lipid bilayers is a common conformation-dependent activity of soluble amyloid oligomers in protein misfolding diseases, *J. Biol. Chem. 279* (45), 46363−46366.
20. Lambert, M. P., Viola, K. L., Chromy, B. A., Chang, L., Morgan, T. E., Yu, J., Venton, D. L., Krafft, G. A., Finch, C. E., and Klein, W. L. (2001) Vaccination with soluble Ab oligomers generates toxicity-neutralizing antibodies, *J. Neurochem. 79*, 595−605.
21. Stafford, W. F. (1992) Boundary Analysis in Sedimentation Transport Experiments: A Procedure for Obtaining Sedimentation Coefficient Distributions Using the Time Derivative of the Concentration Profile, *Anal. Biochem. 203*, 295−301.
22. Philo, J. S. (2000) A method for directly fitting the time derivative of sedimentation velocity data and an alternative algorithm for calculating sedimentation coefficient distribution functions, *Anal. Biochem. 279*, 151−163.
23. Stine, W. B., Jr., Snyder, S. W., Ladror, U. S., Wade, W. S., Miller, M. F., Perun, T. J., Holzman, T. F., and Krafft, G. A. (1996) The nanometer-scale structure of amyloid-β visualized by atomic force microscopy, *J. Protein Chem. 15*, 193−203.
24. Lomakin, A., Chung, D. S., Benedek, G. B., Kirschner, D. A., and Teplow, D. B. (1996) On the nucleation and growth of amyloid β-protein fibrils: Detection of nuclei and quantitation of rate constants, *Proc. Natl. Acad. Sci. U.S.A. 93*, 1125−1129.
25. Oda, T., Wals, P., Osterburg, H. H., Johnson, S. A., Pasinetti, G. M., Morgan, T. E., Rozovsky, I., Stine, W. B., Snyder, S. W., Holzman, T. F., et al. (1995) Clusterin (apoJ) alters the aggregation of amyloid β-peptide (Aβ 1−42) and forms slowly sedimenting Aβ complexes that cause oxidative stress, *Exp. Neurol. 136*, 22−31.
26. Krafft, G. A., Klein, W. L., and Finch, C. E. (2001) Amyloid Beta Protein (Globular assemblies and uses thereof), U.S. Patent 6,218,506.
27. Walsh, D. M., Lomakin, A., Benedek, G. B., Condron, M. M., and Teplow, D. B. (1997) Amyloid β-protein fibrillogenesis. Detection of a protofibrillar intermediates, *J. Biol. Chem. 272*, 22364−22372.
28. Joyce, J. G., Cook, J. C., Przysiecki, C. T., and Lehman, E. D. (1994) Chromatographic separation of low-molecular-mass recombinant proteins and peptides on Superdex-30 prep grade, *J. Chromatogr, Biomed. Appl. 662*, 325−334.
29. Lesne, S., Koh, M. T., Kotilinek, L., Kayed, R., Glabe, C. G., Yang, A., Gallagher, M., and Ashe, K. H. (2006) A specific amyloid-β protein assembly in the brain impairs memory, *Nature 440*, 352−357.
30. Arimon, M., Diez-Perez, I., Kogan, M. J., Durany, N., Giralt, E., Sanz, F., and Fernandez-Busquets, X. (2005) Fine structure study of Aβ1−42. fibrillogenesis with atomic force microscopy, *FASEB J. 19*, 1344−1346.
31. Dahlgren, K. N., Manelli, A. M., Stine, W. B., Jr., Baker, L. K., Krafft, G. A., and LaDu, M. J. (2002) Oligomeric and fibrillar species of amyloid-β peptides differentially affect neuronal viability, *J. Biol. Chem. 277*, 32046−32053.
32. Huang, T. H., Yang, D. S., Plaskos, N. P., Go, S., Yip, C. M., Fraser, P. E., and Chakrabartty, A. (2000) Structural studies of soluble oligomers of the Alzheimer β-amyloid peptide, *J. Mol. Biol. 297*, 73−87.
33. Kowalewski, T., and Holtzman, D. M. (1999) In situ atomic force microscopy study of Alzheimer's β-amyloid peptide on different substrates: New insights into mechanism of β-sheet formation, *Proc. Natl. Acad. Sci. U.S.A. 96*, 3688−3693.
34. Wang, Z., Zhou, C., Wang, C., Wan, L., Fang, X., and Bai, C. (2003) AFM and STM study of β-amyloid aggregation on graphite, *Ultramicroscopy 97*, 73−79.
35. Silva, L. P. (2005) Imaging proteins with atomic force microscopy: An overview, *Curr. Protein Pept. Sci. 6*, 387−395.
36. Ding, T. T., and Harper, J. D. (1999) Analysis of amyloid-β assemblies using tapping mode atomic force microscopy under ambient conditions, *Methods Enzymol. 309*, XXXX.
37. Bitan, G., Fradinger, E. A., Spring, S. M., and Teplow, D. B. (2005) Neurotoxic protein oligomers: What you see is not always what you get, *Amyloid 12*, 88−95.
38. Bitan, G., and Teplow, D. B. (2004) Rapid photochemical cross-linking: A new tool for studies of metastable, amyloidogenic protein assemblies, *Acc. Chem. Res. 37* (6), 357−364.
39. Yanagisawa, K. (2004) A pivotal role of gangliosides in the aggregation of amyloid β-protein in the brain, *Yakugaku Zasshi 124*, 50−52.
40. McLaurin, J., Franklin, T., Fraser, P. E., and Chakrabartty, A. (1998) Structural transitions associated with the interaction of Alzheimer β-amyloid peptides with gangliosides, *J. Biol. Chem. 273*, 4506−4515.
41. Kakio, A., Nishimoto, S., Yanagisawa, K., Kozutsumi, Y., and Matsuzaki, K. (2002) Interactions of amyloid β-protein with various gangliosides in raft-like membranes: Importance of GM1

ganglioside-bound form as an endogenous seed for Alzheimer amyloid, *Biochemistry 41*, 7385−7390.
42. ChooSmith, L. P., GarzonRodriguez, W., Glabe, C. G., and Surewicz, W. K. (1997) Acceleration of amyloid fibril formation by specific binding of Aβ(1−40) peptide to ganglioside-containing membrane vesicles, *J. Biol. Chem. 272*, 22987−22990.
43. Chauhan, A., Ray, I., and Chauhan, V. P. S. (2000) Interaction of amyloid β-protein with anionic phospholipids: Possible involvement of Lys(28) and C-terminus aliphatic amino acids, *Neurochem. Res. 25*, 423−429.
44. Ariga, T., and Yu, R. K. (1999) GM1 inhibits amyloid β-protein-induced cytokine release, *Neurochem. Res. 24*, 219−226.
45. Barghorn, S., Nimmrich, V., Striebinger, A., Krantz, C., Keller, P., Janson, B., Bahr, M., Schmidt, M., Bitner, R. S., Harlan, J., Barlow, E., Ebert, U., and Hillen, H. (2005) Globular amyloid β-peptide oligomer: A homogenous and stable neuropathological protein in Alzheimer's disease, *J. Neurochem.*
46. Kokubo, H., Kayed, R., Glabe, C. G., and Yamaguchi, H. (2005) Soluble Aβ oligomers ultrastructurally localize to cell processes and might be related to synaptic dysfunction in Alzheimer's disease brain, *Brain Res. 1031*, 222−228.
47. Tang, M. K., and Zhang, J. T. (2001) Salvianolic acid B inhibits fibril formation and neurotoxicity of amyloid β-protein in vitro, *Acta Pharmacol. Sin. 22*, 380−384.
48. Hughes, E., Burke, R. M., and Doig, A. J. (2000) Inhibition of toxicity in the β-amyloid peptide fragment β (25−35) using N-methylated derivatives: A general strategy to prevent amyloid formation, *J. Biol. Chem. 275*, 25109−25115.
49. Bergamaschini, L., Donarini, C., Rossi, E., De Luigi, A., Vergani, C., and De Simoni, M. G. (2002) Heparin attenuates cytotoxic and inflammatory activity of Alzheimer amyloid-β in vitro, *Neurobiol. Aging 23*, 531−536.

BI061850F